Mongolian Geoscientist

Review paper

Magnetotelluric studies in Mongolia: Progress status and outlook

Batmagnai Erdenechimeg[1*], Alexey Kuvshinov[2,3]

[1]*Department of Geomagnetism, Institute of Astronomy and Geophysics, Mongolian Academy of Sciences, Ulaanbaatar, 13343, Mongolia*
[2]*Department of Earth and Planetary Sciences, Institute of Geophysics, ETH Zurich, 8092, Switzerland*
[3]*Institute of Solar-Terrestrial Physics, Siberian Branch of Russian Academy of Sciences, Irkutsk, 664033, Russia*

**Corresponding author:* batmagnai@iag.ac.mn, *ORCID:* 0000-0002-1924-182X

ARTICLE INFO

Article history:

Received: 06 February, 2025
Revised: 23 May, 2025
Accepted: 30 May, 2025

ABSTRACT

Mongolia is a unique natural laboratory for studying intracontinental surface deformation and intraplate volcanism due to its location within the high plateaus of the Central Asian Orogenic Belt, far away from active plate margins. The region is also characterized by zones of economically significant mineral deposits and vast geothermal resources, which are intrinsically linked to its lithospheric architecture and crust-mantle interactions. Key earth's properties, such as temperature, fluid content, and partial melt, influence the subsurface electrical conductivity - a target parameter of the magnetotelluric method. Between 2016 and 2024, two large-scale international magnetotelluric projects were conducted, resulting in more than 784 magnetotelluric measurements across a vast area of about 1000×1250 km^2. Additionally, from 2019 to 2023, a focused international magnetotelluric study was carried out at the geothermal field near Tsenkher in the Khangai Mountains, with 256 magnetotelluric measurements over a smaller area of about 35×40 km^2. These projects contributed significantly to understanding the region's lithospheric processes and geothermal systems. Crucially, the knowledge transfer from these collaborative projects has enabled Mongolian researchers to initiate and perform their own magnetotelluric surveys to explore geologically significant areas across the region. This review details performed magnetotelluric surveys (as of the end of 2024), highlights the key results, and discusses potential directions for future research.

Keywords: Electrical conductivity, Inversion, Lithosphere, Geothermal fields, Mineral deposits

INTRODUCTION

Mongolia is located far from tectonic boundaries, deep in the continental interior, but shows recent surface deformation (uplift of Khangai Dome, Central Mongolia) and intraplate volcanism in the region, both remaining unclear and the subject of ongoing debate. Furthermore, there is increasing interest in harnessing Mongolia's sustainable geothermal energy resources to reduce greenhouse gas emissions and improve local air quality. The region is also rich in mineral resources, hosting significant deposits of copper and gold, such as those at the Erdenet, Boroo, and Oyu Tolgoi mines. Prominent tectonic features, including the Mongol-Okhotsk suture zone and the Mogod and Khustai faults, further underscore Mongolia's geological significance. Fig. 1 summarizes the tectonic background and other key information about the region.

A widely used technique to infer the Earth's crust and mantle structure is the magnetotelluric

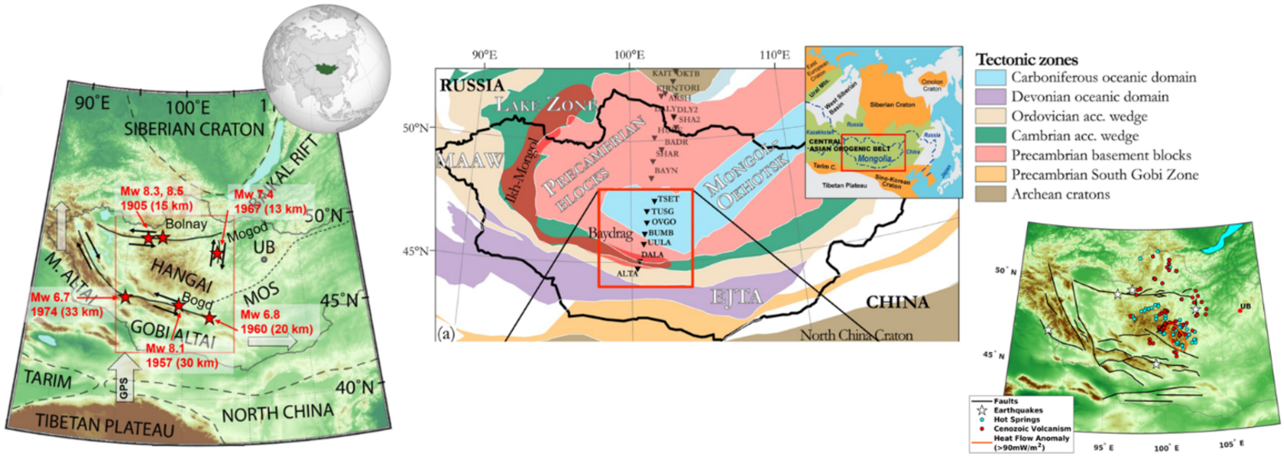

Fig. 1. Tectonic context and other key information. The central plot, adapted from (Guy et al., 2024), provides an overview of the region's tectonic framework. Black arrows in the plot on the left illustrate the seismogenic faults: Bulnai, Bogd, and Mogod. Red stars mark the locations of significant 20th-century earthquakes, with red text indicating their magnitudes, depths, and occurrence years. Broad grey arrows represent the predominant tectonic movements in the region.

(MT) method (Tikhonov, 1950; Cagniard, 1953; Berdichevsky and Dmitriev, 2010), which maps the distribution of electrical conductivity within the Earth's interior, down to depths of around 200 km. Electrical conductivity reflects the connectivity of conductive constituents such as fluids, partial melts, and volatiles and is intrinsically dependent on temperature. Furthermore, MT can also illuminate crustal pathways for magmas and fluids, which are critical for the formation of the mineral deposits and geothermal reservoirs.

MONGOLIAN MT SURVEYS IN A NUTSHELL

Regional scale MT surveys

The first MT survey in Mongolia was launched in 2016 as part of the research project funded through the DACH program of the Swiss National and German Science Foundations. The project brought together scientific teams from ETH Zurich (Switzerland), the University of Münster (UoM; Germany), and the Institute of Astronomy and Geophysics (IAG) of the Mongolian Academy of Sciences (MAS). The primary objective of the project (which we named DACH-1) was to investigate volcanism and the mechanism for the Khangai Dome uplift. Between 2016 and 2018, three field campaigns were conducted in the Khangai and Gobi-Altai regions as part of the project, resulting in MT measurements at 326 sites across a 650×450 km² area. These data include measurements on a regular grid with a site spacing of 50 km and along several profiles with denser site spacing ranging from ~5 to 15 km.

In 2020, the DACH-2 project started, involving the same institutions as its predecessor. This phase focused on investigating geological structures beyond the Khangai Dome. Between 2020 and 2023, five field campaigns were conducted to extend the grid of MT measurements to regions east, west, and north of the Khangai Dome. The site spacing varied from 5 to 50 km, depending on the region and the scale of the features of interest. These campaigns expanded the research area to 1000×1100 km², with MT data collected at 378 sites.

During the 2024 field season, Mongolian researchers collected data at 80 new sites, further expanding the Mongolian MT grid into the eastern regions. As a result, MT data coverage in Mongolia now encompasses an area of 1000×1250 km².

Local scale MT surveys

The first local-scale MT survey in Mongolia was conducted as part of a project funded through the Research for Development (R4D) program of the Swiss National Foundation. Partners in this project were ETH Zurich and IAG MAS. The study focused on investigating the Tsenkher intermediate-temperature geothermal field near

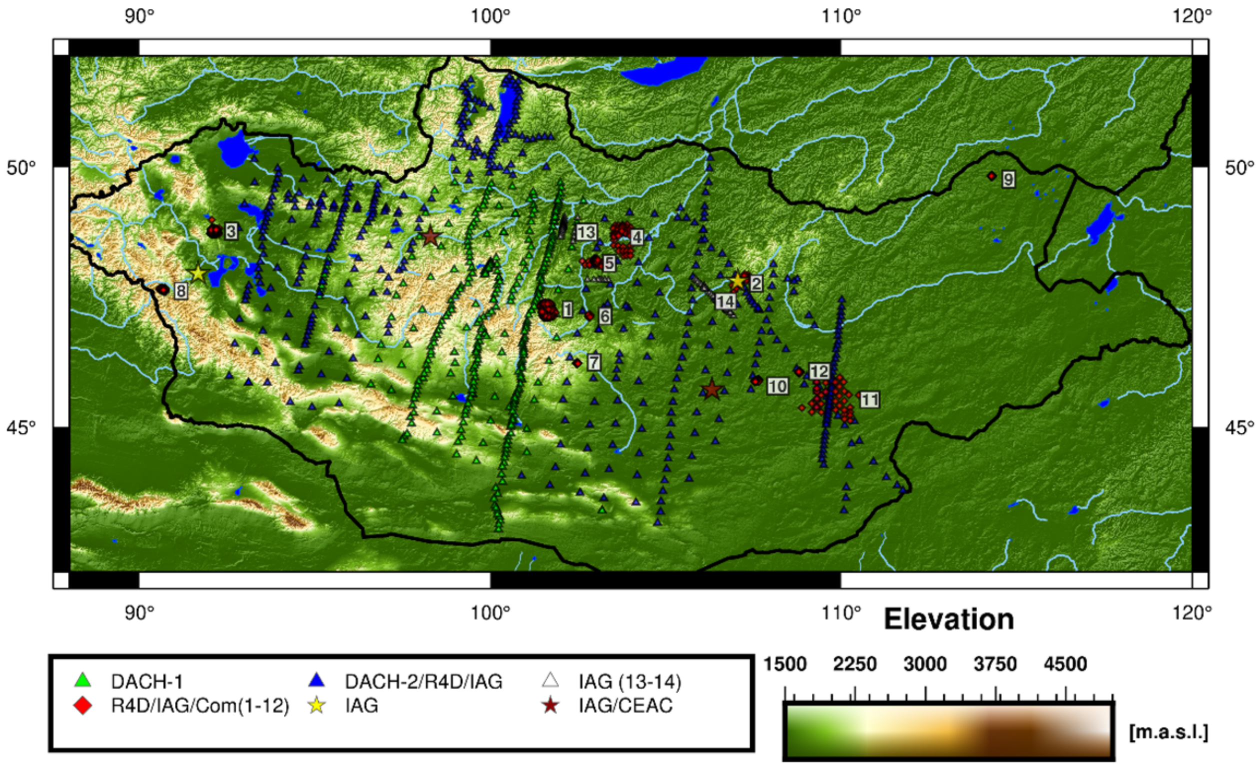

Fig. 2. Distribution of MT sites installed in 2016-2024 years from different projects and surveys. The stars in the figure depict the location of sites/observatories where long-term magnetic field measurements have been performing; yellow stars mark sites run by IAG, and red stars - run by IAG and the Chinese Earthquake Administration Centre (CEAC). The numbers in the brackets (in the legend) correspond to the numbers in the first column of Table 1. The term "Com" in legend means that service companies funded some surveys. See the main text and table for more details.

Table 1. Details on performed regional and local MT surveys. Numbers in brackets in the first column correspond to the numbers in Fig. 2.

Source of funding	Region of interest	Year of surveys	# of sites	Site spacing, km	Area covered, km^2
DACH-1	Khangai Dome (KD) and Gobi Altai (array, profiles)	2016 - 2018	326	5 - 50	650×450
R4D (1)	Tsenkher (array)	2019 - 2020	256	0.5 - 1.5	35×40
DACH-2/R4D/IAG	East, west and north of KD (array, profiles)	2020 - 2024	458	5 - 50	1000×1100
IAG (2)	Ulaanbaatar (array)	2024	18	2 - 5	20×20
IAG (3)	Ulgii (array)	2023	51	0.5 - 2	15×10
Ereen Chuluu (4)	Erdenet (array)	2024	45	10	40×30
IAG (5)	Mogod (array)	2020 - 2022, 2024	77	0.5 - 3	10×8
Asian Development Bank (6)	Kharkhorin (array)	2024	15	1.0 - 2.0	3×3
IAG (7)	Khuremt (array)	2024	38	0.5 - 1	5×5
Copper Investment (8)	Deluun (array)	2024	67	0.5 - 2	5×4
Delta Gold (9)	Dashbalbar (array)	2024	52	0.2 - 1	2×3
Delta Gold (10)	Govi-Ugtaal (array)	2024	83	0.2 - 1	6×3
Hansul (11)	Altanshiree (array)	2024	80	10	50×50
Delta Gold (12)	Dalanjargalan (array)	2024	46	0.2 -1	3×3
IAG (13)	Khanui (profile)	2024	35	0.5 - 1	30×1
IAG (14)	UB Fault (profile)	2024	45	0.5 - 5	130×1

Tsetserleg city in the Khangai Mountains. Grid-based MT measurements were carried out by the IAG team in 2019 and 2020 at 256 sites, with site spacing ranging from 0.5 to 1.5 km, covering an area of approximately 35×40 km². The data were collected using the pool of eight MT instruments procured for the IAG through the R4D project. Notably, between 2021 and 2024, Mongolian researchers used these instruments to collect data for the regional MT surveys discussed earlier. Currently, the instruments are routinely used by the IAG team to perform nationally supported regional and local MT surveys. Fig. 2 shows the distribution of MT sites installed in 2016-2024 years, and Table 1 details MT surveys performed.

KEY RESULTS OF THE MT STUDIES PERFORMED

We present the results as summaries of papers organized in chronological order. The reader can also find excerpts from the papers (in the form of key figures) in Appendix E to this paper. In addition, Appendices A-D include information about transfer functions (TF) used in MT (Appendix A), instruments to record MT field (Appendix B), approaches to estimate MT TF (Appendix C), and invert estimated TF (Appendix D).

Comeau et al. (2018) and Käufl et al. (2020) utilized MT data collected as part of the DACH-1 project to generate 2-D and 3-D electrical resistivity models of the Khangai Dome and its surroundings. The models revealed a highly resistive upper crust, attributed to a Precambrian cratonic basement with several low-resistivity features. These features were interpreted as late Cenozoic volcanic zones and modern geothermal areas, which appear connected to mantle structures, as well as major fault systems marking terrane boundaries and mineralized zones. In the lower crust, the models identified discrete east-west trending zones of low-resistivity material, indicating the presence of fluids and a mechanically weakened crust. A striking feature in the models is a large low-resistivity zone detected in the upper mantle. This zone suggests a non-uniform lithosphere-asthenosphere boundary with localized upwellings that extend to a depth of 70 km. The laterally inhomogeneous low-resistivity zone is consistent with the presence of partial melt (>3.5%) within an asthenospheric upwelling, which is thought to drive intraplate volcanism and contribute to regional uplift (see Fig. E1, Appendix E).

Comeau et al. (2020a) generated a 2-D model of the region, which extends 350 km from Khangai Dome across the Gobi-Altai Mountains to the Mongolia-China border. The model shows a generally resistive upper crust with several anomalously conductive features that are believed to indicate suture zones and the boundaries of tectonic zones (see Fig. E2a, Appendix E). Moreover, their spatial distribution coincides with known surface fault segments and active seismicity. The lower crust becomes generally less resistive but contains an anomalously conductive feature below the Gobi-Altai zone. Furthermore, due to their unique tectonic histories, there is a large contrast in the electrical properties between identified tectonic zones. The results also indicate a thick lithosphere below Southern Mongolia (>100 km), in contrast to the thin lithosphere below Khangai Dome. Moreover, it is suggested that a steep lithospheric step may exist below the Gobi-Altai Mountains, highlighting the importance of this region as a major lithospheric boundary within the Central Asian Orogenic Belt (CAOB).

Comeau et al. (2020b) presented 2-D models of the crust beneath the Bulnay region, revealing a pattern of discrete low-resistivity zones (~25 km wide) in the lower crust. The authors proposed a conceptual model in which fluid localization and stagnation occur due to thermally activated compaction and demonstrated it is compatible with the observed low-resistivity zones. The model explains the location, shape, and size of the zones, with plausible values of the activation energy for lower crustal creep and a viscous compaction length of approximately 10 km. Comeau et al. (2020b) suggest that rather than lithological or structural heterogeneity, tectonic deformation and compaction processes primarily control regional fluid flow in the lower crust (see Fig. E2b, Appendix E).

Comeau et al. (2021a) and Comeau et al. (2021b) imaged the crustal structure beneath a metallogenic belt and its surroundings in the Bayankhongor area, which hosts essential mineralization zones, including copper and gold deposits. The authors analyzed MT data acquired across this region and produced 3-D models of the crustal structure, which is locally highly heterogeneous. Notably, anomalous low-resistivity zones align with the suture zone and ophiolite belt, identifying them as major crustal-scale features. Furthermore, broadening low-resistivity zones located down-dip from the suture zone suggest that the narrow deformation zone observed at the surface transitions to a wide area in the deeper crust. Based on the available evidence, the observed low resistivity in both cases was attributed to hydrothermal alteration along fossil fluid pathways. The results demonstrate that the crustal architecture - including the major crustal boundary - acts as a first-order control on the location of the metallogenic belt (see Fig. E3, Appendix E).

Comeau et al. (2021c) performed geodynamic modeling of Central Mongolia and showed that slab break-off or delamination of a thickened and stable lithosphere after prolonged subduction processes would increase the hot asthenosphere's upwelling and partial decompression melting, consistent with intraplate volcanism. Ultimately, their results suggest that lithospheric removal by delamination is a physically plausible mechanism and a potential explanation for intraplate uplift.

Comeau et al. (2022a) generated and analyzed 2-D models of the structure beneath the Tariat and Chuluut volcanic zones with the goal of imaging the volcanic system from surface to mantle source. The models revealed narrow, subvertical, low-resistivity anomalies in the middle-to-upper crust, notably aligned with surface expressions of volcanism (see Fig. E4a-b, Appendix E). The lower crust is characterized by the widespread distribution of isolated low-resistivity zones. Additionally, a localized low-resistivity zone was imaged in the mantle at depths of 60-90 km, situated above a broad, homogeneous, doming low-resistivity feature. The authors interpreted the middle-to-upper crustal anomalies as remnant signatures of transient magma pathways or collections of pathways formed by metasomatic alteration during the ascent of hot magmatic fluids. The lower crustal anomalies were attributed to domains of saline fluids within a thermally perturbed lower crust. In the mantle, the low-resistivity structure was explained by a broad mantle upwelling and thermal anomaly, with a localized zone of low-percent partial melt acting as the source of intraplate volcanism.

Comeau et al. (2022b) investigated the whole-lithosphere structure of a gold and copper metallogenic belt located south of the Khangai Dome. The study analyzed geophysical signatures by examining 3-D models of electrical resistivity and shear-wave velocity which had been generated in earlier research. Directly beneath the metal belt, narrow, vertical, finger-like low-resistivity features were identified within the resistive upper-to-middle crust, connected to a large low-resistivity zone in the lower crust. In the lithospheric mantle, a broad low-resistivity zone was imaged, aligning well with a zone of low shear-wave velocity, as confirmed by correlation analysis. In the upper-to-middle crust, the resistivity signatures provide evidence for ancient fluid pathways constrained by a structure along a tectonic boundary. In the lower crust, the resistivity and velocity signatures were interpreted to represent a fossil fluid source region (see Fig. E4c, Appendix E). The authors proposed that these signatures resulted from a combination of factors related to re-fertilization and metasomatism of the lithospheric mantle by long-lived subduction at the craton margin, possibly including iron enrichment, F-rich phlogopite, and metallic sulfides.

Comeau et al. (2024a) analyzed and inverted profile MT data across the Mongol-Okhotsk suture and the Adaatsag ophiolite belt, which are associated with the closure of the Mongol-Okhotsk paleo-ocean and situated within the CAOB and Mongolia. The northern segment of the generated 2-D model reveals a sharp transition from a high-resistivity upper crust to a low-resistivity lower crust, similar to the structure observed beneath the Khangai Dome. In contrast, this transition is absent in the southern segment. A broad, low-resistivity zone imaged in the crust and lithospheric mantle aligns with the Mongol-Okhotsk suture and ophiolite, revealing a distinct lithospheric-scale feature. Across the profile, numerous narrow, vertically oriented, low-resistivity structures are spatially associated remarkably well with the proposed boundaries of tectonic domains. Some of these low-resistivity features are beneath the surface locations of large mineral zones and likely represent fossil fluid pathways (see Fig. E5a, Appendix E).

Rigaud et al. (2023) and Rigaud et al. (2024) generated a new regional 3-D resistivity model across Mongolia using MT data collected from most grid and profile sites. The model encompasses the Khangai Dome and vast regions to the west and east of the Dome. The model reveals a north-south dichotomy across Mongolia, with a clear boundary at crustal depths. In the central/eastern regions, it is defined by east-west trending anomalies, which follow the Main Mongolian Lineament (MML) in the west, the boundary is defined by northwest-southeast to north-south oriented structures following Ikh-Mongol terrane (see Fig. E5b, Appendix E). As discussed earlier, Comeau et al. (2018) and Käufl et al. (2020) detected an upper mantle low-resistivity anomaly underneath the Khangai Dome and interpreted it as a non-uniform lithosphere-asthenosphere boundary with localized upwellings. A new 3-D model reveals that the anomaly is not only restricted to the Dome but is imaged in western/central regions bounded to the south by the MML and to the east by a resistive anomaly whose location coincides with the Mogod fault. This resistive anomaly also separates regions with distinct conductivity patterns within the lower crust and mantle, with the anomalies to the west of this feature being of a larger scale than those located to the east. This may indicate different lithospheric blocks bounded by this fault system.

A series of works (Erdenechimeg et al., 2019, 2020; Erdenechimeg, 2023) present details on and discuss the results of the first 3-D MT study aiming to explore the Tsenkher intermediate-temperature geothermal field. This area features three hot springs, with fluid discharge rates reaching up to 10 liters per second and temperatures as high as 87°C. The 3-D resistivity model generated in this study reveals a narrow low-resistivity anomaly that transects a topographic high between two hot spring areas. The authors interpreted this anomaly as a permeable zone of topography-driven and fault-controlled deep fluid circulation in a radiothermal granite delineating the source region and thermal water reservoirs. The model offers insight into the geophysical signatures of geothermal resource formation at the Tsenkher hot springs area and lays the foundations for developing geothermal energy projects. The study further demonstrates that 3-D MT subsurface imaging is a viable and valuable tool for localizing deep fluid circulation zones and providing key information for exploring intermediate-temperature geothermal systems (see Fig. E6a, Appendix E).

In another series of studies (Enkhzul and Batmagnai, 2021, Enkhzul et al., 2021, 2022), IAG researchers utilized the MT method to investigate the Mogod region, known for its geothermal and seismic activity, to better understand its internal structure. Initial inversion results revealed prominent vertical low-resistivity features, which may correspond to the deep roots of local geological activation (see Fig. E6b, Appendix E).

Finally, Comeau et al. (2024b) obtained a 2-D resistivity model of the region west of Ulaanbaatar, an area characterized by active faults capable of generating high-magnitude earthquakes, posing a significant risk to the Mongolian capital. Analysis of this model provides insights into the subsurface structure of the region and enhances the characterization of active faults, representing an important step in assessing seismic hazards.

CONCLUDING REMARKS AND OUTLOOK

This paper provides an overview of the current (end of 2024) status of MT studies in Mongolia, which began from scratch in 2016. Over the past nine years, significant progress in acquiring, processing, inverting, and interpreting the MT data has been achieved through collaborative efforts under three international projects. Collected MT data appeared to be of exceptionally high quality due to very low cultural/industrial noise in the region.

A substantial part of MT measurements has been conducted on a regular grid with a site spacing of approximately 50 km, wherever feasible. As of 2024, approximately half of Mongolia is covered by grid measurements. In addition to the grid-based surveys, denser-spacing measurements were carried out along eight predominantly north-south-oriented profiles. These data have enabled researchers to characterize the properties and architecture of Mongolia's lithosphere at multiple scales and dimensions using innovative acquisition layouts and state-of-the-art inverse tools. Furthermore, fourteen local MT surveys have been undertaken to investigate smaller-scale features of both scientific and economic interest, including fault systems, mineral deposits, and geothermal fields. To date, more than 1600 MT sites have been deployed across an area of approximately 1000 km by 1250 km, similar in scope to other national MT survey programs such as the EMScope in the United States (Schultz et al., 2010), AusLAMP in Australia (Tiel et al., 2020), and SinoProbe in China (Jin et al., 2022).
Based on the analysis of the collected and processed data, 15 papers have already been published, with more publications forthcoming. However, from our perspective, one of the most significant achievements of the nine-year MT initiative in Mongolia is the establishment of the electromagnetic (EM) lab at the Institute of Astronomy and Geophysics, MAS. The lab is headed by Dr. Batmagnai Erdenechimeg, the first co-author of this paper, who received his doctoral degree from ETH Zurich, Switzerland, in 2023. Today, the EM lab research team possesses extensive expertise in conducting comprehensive MT studies, encompassing everything from data acquisition to interpreting MT inversion results. The lab is equipped with eight modern broadband MT instruments (with an additional four instruments to come in 2025), enabling Mongolian researchers to independently carry out MT surveys across a wide range of scales, from local to regional. Notably, establishing a dedicated laboratory for MT/EM research marks a significant accomplishment, as, to our knowledge, only a few national research institutes worldwide have similar facilities.

The envisaged goal for the EM lab in 2025-2026 years is to complete gridded MT measurements with a site spacing of 50 km across all of Mongolia. This effort forms part of the proposed scientific project MARMOT (Mongolian ARray of MagnetOtelluric and Telluric observations). In the second phase of the project (2027-2030), it is planned to conduct array MT measurements on a denser grid with a site spacing of 25 km. This advancement will enable researchers to acquire detailed information on the Central Asian Orogenic Belt (CAOB) and its formation while also aiding in discovering new mineral deposits and geothermal reservoirs across Mongolia.
To investigate structures at mantle (greater than 200 km) depths, where the MT method has limited resolution, the geomagnetic depth sounding (GDS) technique (Kuvshinov, 2012) is planned to be employed. As is known, GDS relies on continuous, long-term measurements of a time-varying magnetic field. Since 1965, such measurements have been conducted at a geomagnetic observatory southeast of Ulaanbaatar. Since 2003, continuous magnetic field measurements have been carried out in Khovd, western Mongolia. In 2024, the Chinese Earthquake Administration Centre in cooperation with IAG, established two geomagnetic observatories in Mandalgovi (southern Mongolia) and Tosontsengel (northwestern Mongolia) as part of the One Belt and Road project. The locations of these geomagnetic observatories are shown in Fig. 2. The data from these observatories provide a unique opportunity to enhance our understanding of mantle structures beneath Mongolia.
For detailed studies of very shallow structures associated with mineral deposits and geothermal reservoirs, an attractive alternative to MT is the controlled-source electromagnetic (CSEM) method (Ziolkowski and Slob, 2019). Efforts are underway to gather information on available CSEM instrumentation and methodological solutions and develop expertise in conducting CSEM surveys and processing/interpreting CSEM data.
Ultimately, all data collected during the surveys discussed above and upcoming ones will be

processed in a unified manner, stored in an open-access repository, and inverted using a multi-scale and multi-source inversion framework. This approach will enable researchers to image the internal structure of the entire Mongolia from the surface down to the mid-mantle. Finally, an outstanding goal is to perform joint interpretation of EM results and results from other geophysical methods, including seismology, gravimetry, and magnetometry.

With these ambitious goals in mind, the EM Lab's crucial priority is recruiting and training junior scientists to collect, process, analyze, invert, and interpret existing and emerging data.

ACKNOWLEDGEMENTS

We thank all those who participated in and provided support in collecting, processing, and inverting Mongolian MT data and interpreting the results of inversions. They include (in alphabetical order for each institution) Luise Dambly, Alexander Grayver, Sandra Grazioli, Johannes Kauefl, Rafael Rigaud, Martin Saar, Friedemann Samrock, Dorian Sorgel, Neeraj Sudhir from ETH Zurich, Switzerland; Michael Becken, Dominic Harpering, Phillip Kotowski, Robin Mann, Johanna Plett, Jorg Schmalzl, Hannah Treppke from University of Muenster, Germany; Matthew Comeau from Delft University of Technology, Delft, The Netherlands; Mikhail Kruglyakov from University of Otago, New Zealand; Batbileg Tegshjargal, Bayrjargal Bizya, Demberel Sodnomsambuu, Eldev-Ochir Bold, Gantsogt Sukhbaatar, Nasan-Ochir Tumen, Nomuun Narantsogt, Odonbaatar Chimed, Sukhbaatar Usnikh, Tsagaansukh Khalzaa, Tserendug Shoovdor, Tuwshin Otgon, Zagdsuren Shatar and the staff of local seismic observatories from Institute of Astronomy and Geophysics, Mongolian Academy of Sciences.

REFERENCE

Berdichevsky, M.N., Dmitriev, V.I. 2010. Models and methods of magnetotellurics. Springer Springer Berlin, Heidelberg, 564 p. https://doi.org/10.1007/978-3-540-77814-1

Cagniard, L. 1953. Basic theory of the magneto-telluric method of geophysical prospecting. Geophysics, vol. 18(3), p. 605-635. https://doi.org/10.1190/1.1437915

Comeau, M.J., Batmagnai, E., Tserendug, Sh., Bayartogtokh, E., Kuvshinov, A., Demberel, S. 2024b. Implications for seismic hazard assessment from the characterization of active fault zones near Ulaanbaatar with electrical resistivity models. Abstracts of the 26th International Electromagnetic Induction Workshop 2024, Beppu, Japan.

Comeau, M.J., Becken, M., Connolly, D., Grayver, A.V., Kuvshinov, A. 2020b. Compaction-Driven Fluid Localization as an Explanation for Lower Crustal Electrical Conductors in Intracontinental Setting. Geophysical Research Letters, vol. 47(19), e2020GL088455. https://doi.org/10.1029/2020GL088455

Comeau, M.J., Becken, M., Grayver, A.V., Käufl, J.S., Kuvshinov, A.V. 2022a. The geophysical signature of a continental intraplate volcanic system: From surface to mantle source. Earth and Planetary Science Letters, v. 578, 117307. https://doi.org/10.1016/j.epsl.2021.117307

Comeau, M.J., Becken, M., Käufl, J.S., Grayver, A.V., Kuvshinov, A.V., Tserendug S., Batmagnai, E., Demberel, S. 2020a. Evidence for terrane boundaries and suture zones across Southern Mongolia detected with a 2-dimensional magnetotelluric transect. Earth, Planets and Space, vol. 72, p. 1-13, https://doi.org/10.1186/s40623-020-1131-6

Comeau, M.J., Becken, M., Kuvshinov, A.V. 2022b. Imaging the Whole-Lithosphere Architecture of a Mineral System - Geophysical Signatures of the Sources and Pathways of Ore-Forming Fluids. Geochemistry, Geophysics, Geosystems, vol. 23(8), e2022GC010379. https://doi.org/10.1029/2022GC010379

Comeau, M.J., Becken, M., Kuvshinov, A.V., Demberel, S. 2021a. Crustal architecture of a metallogenic belt and ophiolite belt: Implications for mineral genesis and emplacement from 3-D electrical resistivity models (Bayankhongor area, Mongolia). Earth, Planets and Space, vol. 73, p. 1-20, https://doi.org/10.1186/s40623-021-01400-9

Comeau, M.J., Käufl, J.S., Becken, M.,

Kuvshinov, A., Grayver, A.V., Kamm, J., Demberel, S., Sukhbaatar, U., Batmagnai, E. 2018. Evidence for fluid and melt generation in response to an asthenospheric upwelling beneath the Hangai Dome, Mongolia. Earth and Planetary Science Letters, vol. 487, p. 201-209. https://doi.org/10.1016/j.epsl.2018.02.007

Comeau, M.J., Rigaud, R., Batmagnai, E., Tserendug, Sh., Kuvshinov, A., Becken, M., Demberel, S. 2024a. Insights into the structure of the Mongol-Okhotsk suture zone, Adaatsag ophiolite, and tectonic boundaries of the Central Asian Orogenic Belt (Mongolia) from electrical resistivity imaging and seismic velocity models. Journal of Geophysical Research: Solid Earth, vol. 129(4), e2023JB028503. https://doi.org/10.1029/2023JB028503

Comeau, M.J., Becken, M., Kuvshinov, A.V., Demberel, S., Batmagnai, E., Tserendug, S. 2021b. Investigating the Whole-lithosphere Structure of a Mineral System-Pathways and Source of Ore-forming Fluids Imaged with Magnetotelluric Modeling. Acta Geologica Sinica (English Edition), vol. 95(S1), p.73-75 https://doi.org/10.1111/1755-6724.14837

Comeau, M.J., Stein, C., Becken, M., Hansen, U. 2021c. Geodynamic Modelling of Lithospheric Removal and Surface Deformation: Application to Intraplate Uplift in Central Mongolia. Journal of Geophysical Research: Solid Earth, vol. 126(5), e2020JB021304. https://doi.org/10.1029/2020JB021304

Egbert, G.D., Kelbert, A. 2012. Computational recipes for electromagnetic inverse problems. Geophysical Journal International, vol. 189(1), p. 251-267. https://doi.org/10.1111/j.1365-246X.2011.05347.x

Enkhzul, B., Batmagnai, E. 2021. 1-D MT inversion using by deterministic inversion technique. Journal of Astronomy and Geophysics, Institute of Astronomy and Geophysics, Mongolian Academy of Sciences, vol. 8, p. 94-105 (in Mongolian) https://iag.mn/file/Journals/Setguul_N8.pdf

Enkhzul, B., Batmagnai, E., Tserendug, S., Bayanjargal, G. 2022. Investigation of the electrical resistivity structure of the subsurface at Mogod valley in central Mongolia: Insight is using 1D magnetotelluric inversion. Mongolian Geoscientist vol. 27(54), p. 37-50. https://doi.org/10.5564/mgs.v27i54.1810

Enkhzul, B., Tserendug, Sh., Batmagnai, E. 2021. MT signal processing and modeling: implementation for LEMI-423 MT stations. Journal of Astronomy and Geophysics, Institute of Astronomy and Geophysics, Mongolian Academy of Sciences, vol. 8, p. 106-118 (in Mongolian) https://iag.mn/file/Journals/Setguul_N8.pdf

Erdenechimeg, B. 2023. Magnetotelluric exploration of intermediate temperature geothermal systems and mineral resources in central Mongolia. Doctoral Thesis. ETH Zurich, 293 p. https://doi.org/10.3929/ethz-b-000623203

Erdenechimeg, B., Samrock, F., Grayver, A., Kuvshinov, A., Saar, M.O., Sodnomsambuu, D., Shoovdor, T., Dorj, P. 2022. Using MT for understanding the formation of nonvolcanic geothermal systems: case study from Tsenkher geothermal area in Mongolia, Abstracts of the 25th EM induction workshop, Çeşme, Turkey, September 11-17, 2022, https://doi.org/10.3929/ethz-b-000595695

Erdenechimeg, B., Samrock, F., Grayver, A.V., Kuvshinov, A., Saar, M.O., Sodnomsambuu, D., Battuulai, T., Shoovdor, T., Dorj, Purevsuren., Dolgorsuren, O. 2019. Integrated geoscientific exploration for geothermal energy utilization in the Mongolian Hangai. Geophysical Research Abstracts, vol. 21, EGU2019-8983. https://doi.org/10.3929/ethz-b-000392518

Erdenechimeg, B., Samrock, F., Grayver, A.V., Kuvshinov, A., Saar, M.O., Sodnomsambuu, D., Battuulai, T., Shoovdor, T., Dorj, Purevsuren., Dolgorsuren O. 2020. 3-D magnetotelluric investigation of the mid-enthalpy geothermal region near Tsetserleg city in Mongolian Arkhangai province. AGU Fall Meeting 2020, Abstract GP007-0011. 2020AGUFMGP0070011E

Grayver, A.V. 2015. Parallel three-dimensional magnetotelluric inversion using adaptive finite-element method. Part I: theory and synthetic study. Geophysical Journal International, vol. 202(1), p. 584-603.

https://doi.org/10.1093/gji/ggv165

Guy, A., Tiberi, C., Mijiddorj, S. 2024. Crustal structures from receiver functions and gravity modeling in central Mongolia. Journal of Geophysical Research: Solid Earth, vol. 129(1), e2023JB027614. https://doi.org/10.1029/2023JB027614

Harpering, D. 2018. Robust processing scheme for magnetotelluric data. MSc dissertation; University of Münster.

Hermance, J.F., Thayer, R.E., 1975. The telluric-magnetotelluric method. Geophysics, vol. 40(4), p. 664-668. https://doi.org/10.1190/1.1440557

Huber, P.J., Ronchetti, E.M. 2009. Robust Statistics (2nd ed.). Hoboken, NJ: John Wiley & Sons Inc. 354 p. https://onlinelibrary.wiley.com/doi/book/10.1002/9780470434697

Jin, S., Sheng, Y., Comeau, M.J., Becken, M., Wei, W., Ye, G., Dong, H., Zhang, L. 2022. Relationship of the crustal structure, rheology, and tectonic dynamics beneath the Lhasa-Gangdese Terrane (Southern Tibet) based on a 3-D electrical model. Journal of Geophysical Research: Solid Earth, vol. 127(11), e2022JB024318. https://doi.org/10.1029/2022JB024318

Kalscheuer, T., Juanatey, M., Meqbel, N., Pedersen, L.B. 2010. Non-linear model error and resolution properties from two-dimensional single and joint inversions of direct current resistivity and radiomagnetotelluric data. Geophysical Journal International, vol. 182(3), p. 1174-1188. https://doi.org/10.1111/j.1365-246X.2010.04686.x

Käufl, J.S., Grayver, A.V., Comeau, M.J., Kuvshinov, A.V., Becken, M., Kamm, J., Batmagnai, E., Demberel, S. 2020. Magnetotelluric multi-scale 3-D inversion reveals crustal and upper mantle structure beneath the Hangai and Gobi-Altai regions in Mongolia. Geophysical Journal International, vol. 221(2), p. 1002-1028. https://doi.org/10.1093/gji/ggaa039

Key, K. 2016. MARE2DEM: a 2-D inversion code for controlled-source electromagnetic and magnetotelluric data. Geophysical Journal International, vol. 207(1), p. 571-588. https://doi.org/10.1093/gji/ggw290

Kuvshinov, A. 2012. Deep Electromagnetic Studies from Land, Sea, and Space: Progress Status in the Past 10 years. Survey in Geophysics, vol. 33, p. 169-209. https://doi.org/10.1007/s10712-011-9118-2

Rigaud, R. 2024. Regional magnetotelluric study across Mongolia: Constraining lithospheric properties and architecture. Doctoral Thesis. ETH Zurich, 223 p. https://doi.org/10.3929/ethz-b-000709100

Rigaud, R., Comeau, M.J, Becken, M., Kuvshinov, A.V, Tserendug, S., Batmagnai, E., Demberel, S. 2023. Magnetotelluric Data Across Mongolia: Implications for Intracontinental Deformation and Intraplate Volcanism - Report on New Measurements, EGU General Assembly 2023, Vienna, Austria, 24-28 April 2023, EGU23-9485. https://doi.org/10.5194/egusphere-egu23-9485

Schultz, A. 2010. EMScope: a continental scale magnetotelluric observatory and data discovery resource, Data Science Journal, vol. 8, IGY6–IGY20. https://doi.org/10.2481/dsj.SS_IGY-009

Tikhonov, A.N. 1950. On determining electrical characteristics of the deep layers of the Earth's crust: in Doklady Akademii Nauk, v. 73, p. 295-297 (in Russian).

Thiel, S., Goleby, B.R., Pawley, M.J. Heinson, G. 2020. AusLAMP 3D MT imaging of an intracontinental deformation zone, Musgrave Province, Central Australia. Earth, Planets and Space, vol.72(98). https://doi.org/10.1186/s40623-020-01223-0

Ziolkowski, A., Slob, E. 2019. Introduction to Controlled-Source Electromagnetic Methods: Detecting Subsurface Fluids. Cambridge University Press. https://doi.org/10.1017/9781107415904

APPENDIX A:

MT TRANSFER FUNCTIONS

The MT method is based on the assumption that the (natural) source of the time-varying electromagnetic (EM) field is located far above the Earth's surface in a way that the source EM field at the surface is observed as a vertically propagating laterally uniform plane wave of varying polarization. This assumption is valid for the EM field variations with periods up to a few hours in non-polar regions. Following the skin depth concept, the MT field penetrates deeper into the Earth with the decreasing frequency of the MT variations and/or decreasing the electrical conductivity of the Earth. The Earth's response to the source excitation is described by frequency-dependent, complex-valued transfer functions (TFs), which carry information about the distribution of electrical conductivity in the subsurface. The main steps of the MT technique include: a) recording temporal variations of magnetic and electric fields in the region of interest, b) estimation from these data MT transfer functions, and c) inversion of these TFs in terms of subsurface electrical conductivity. The primary TF in MT is the impedance Z that relates horizontal electric and magnetic field as

$$\mathbf{E}_h(\mathbf{r},\omega) = Z(\mathbf{r},\omega)\mathbf{H}_h(\mathbf{r},\omega) \tag{A1}$$

Here is ω -the angular frequency, $\mathbf{E}_h = (E_x, E_y)^T$ and $\mathbf{H}_h = (H_x, H_y)^T$ are the Fourier transforms of the corresponding components at a location $\mathbf{r} = (x, y, z)$, where x- and z- axes are directed to geomagnetic (or geographic) north and east, respectively, and z - axis is downward directed. The MT impedance is the second-order tensor written as

$$Z(\mathbf{r},\omega) = \begin{pmatrix} Z_{xx}(\mathbf{r},\omega) & Z_{xx}(\mathbf{r},\omega) \\ Z_{yx}(\mathbf{r},\omega) & Z_{yy}(\mathbf{r},\omega) \end{pmatrix} \tag{A2}$$

As can be seen, the (single-site) impedance tensor is estimated using an electric and magnetic field time series measured at the same location $\mathbf{r}$. The alternative transfer function is the inter-site impedance, Z_i (Hermance and Thayer, 1975) defined as

$$\mathbf{E}_h(\mathbf{r},\omega) = Z_i(\mathbf{r},\mathbf{r}_b,\omega)\mathbf{H}_h(\mathbf{r},\mathbf{r}_b,\omega) \tag{A3}$$

where Z_i is estimated from the electric field measured at the location $\mathbf{r}$ and the magnetic field measured at the location $\mathbf{r}_b$ (denoted as base site).

APPENDIX B:

INSTRUMENTS USED IN MONGOLIAN MT SURVEYS

A variety of MT instruments were used to perform 2016-2024 MT surveys. Table B summarizes information about them.

Table B. Details on instruments used in Mongolian MT surveys. BB stands for broad-band measurements of electric and magnetic fields when the magnetic field is recorded using induction coil sensors; BB measurements allow for estimating MT transfer functions (TF) in the frequency band 100 Hz - 0.0001 Hz. LP stands for long-period measurements of electric and magnetic fields when the magnetic field is recorded using fluxgate sensors; LP measurements allow for estimating MT TF in the frequency band 0.01 Hz - 0.00001 Hz. BB/LP stands for electric field measurements only, allowing for estimating TF in the frequency band 100 Hz - 0.00001 Hz.

Instruments	BB or/and LP	Sampling, Hz	Years of use
Spam4, GFZ Potsdam, Germany	BB	500	2016, 2017
EDL, United Kingdom	LP	2	2016
EDE, UoM, Germany	BB/LP	500	2016-2023
ADU-07, Metronix, Germany	BB	500	2018, 2023
LEMI 423, Ukraine	BB	500	2019-2024
LEMI 423E, Ukraine	BB/LP	500	2019-2024
GeoMag-02, Ukraine	LP	1	Since 2023

APPENDIX C:

ESTIMATING MT TRANSFER FUNCTIONS

MT single-site and inter-site impedances at each MT site and each frequency/period were estimated from the measured time series of the MT field using a robust processing tool (Harpering, 2018) which exploits windowed Fourier transforms and is based on the M-estimator (e.g., Huber and Ronchetti, 2009). To maximize the quality of the estimates (i.e., make them smoother with respect to periods and decrease their uncertainty) and also extend the period range of TF, processing parameters (such as time windows selection, their length, coherence threshold values, and base site selection for inter-site impedance estimation) were optimized for each station individually.

APPENDIX D:

INVERSION OF MT TRANSFER FUNCTIONS

MT inversion implies the recovery of the subsurface conductivity distribution from the MT TF estimated from the data collected in a given survey area. The (non-linear) MT inversion is formulated as a minimization task, expressed as

$$\mathrm{F}(\mathbf{m}) = \mathrm{F}_d(\mathbf{d},\mathbf{m}) + \lambda \mathrm{F}_m(\mathbf{m}) \underset{\mathbf{m}}{\rightarrow} \min , \qquad \text{(D1)}$$

where F_d is the data misfit, F_m the regularization term, $\mathbf{d}$ the data vector (comprising MT TF at given sets of MT sites and frequencies), $\mathbf{m}$ the vector of model parameters describing the conductivity distribution to be recovered, and λ the regularization parameter, which narrows a class of feasible conductivity distributions. When the recovery of 2-D or 3-D conductivity distribution is required, iterative gradient-based techniques such as Gauss- or quasi-Newton methods are commonly used to minimize functional in eq. (D1). The iterative process involves multiple runs of MT forward modelling. Forward modelling means computing the electric and magnetic fields at observation sites and specified frequencies in a model with a given conductivity distribution excited by a plane wave source of two orthogonal polarizations. The computed fields are then used to calculate (model) MT TF. Since MT electric and magnetic fields obey Maxwell's equations, their computation relies on a numerical solution of these equations. Three basic numerical simulation techniques for computing 2-D/3-D MT fields and responses are finite-difference (FD), finite element (FE), and integral equation (IE) methods. Table D provides details on inverse solvers used in Mongolian MT studies, including, in particular, which simulation techniques were used in which solver.

Table D. Details on numerical solvers used in different papers to invert Mongolian MT data. The solvers EMILIA, Mare2DEM, ModEM, GOFEM, and GEMMIE solvers are introduced in the respective papers (Kalscheuer et al., 2010; Key, 2016; Egbert and Kelbert, 2012; Grayver, 2015, Rigaud, 2024).

Name of inverse solver	Method to simulate EM field	Model dimension (2-D/3-D)	Open access (Yes/No)	Papers/abstracts in which the solver was used
EMILIA	FD	2-D	No	Comeau et al. (2018, 2022a)
Mare2DEM	FE	2-D	Yes	Comeau et al. (2020a, 2022b, 2024a, 2024b)
GOFEM	FE	3-D	No	Käufl et al. (2020), Erdenechimeg et al. (2019, 2020)
ModEM	FD	3-D	Yes	Comeau et al. (2021a)
GEMMIE	IE	3-D	Yes	Rigaud, 2024 and Rigaud et al. (2024)

APPENDIX E:

MT MODELS AND CORRESPONDING INFORMATION MONGOLIAN MT PAPERS

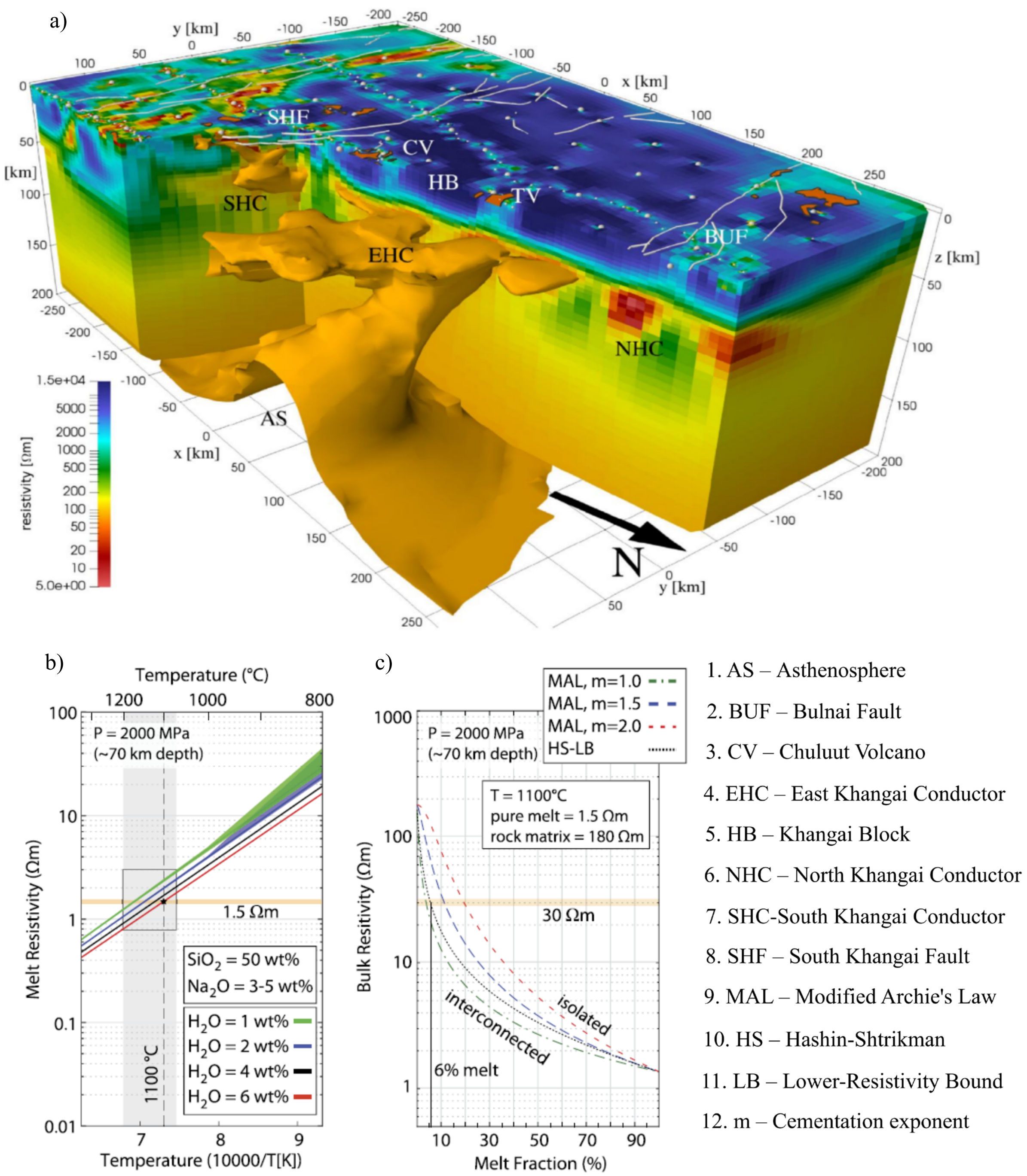

Fig. E1. a) Cutaway of the 3-D electrical resistivity model of Central Mongolia; abbreviations of the recovered structures are deciphered in the right bottom list (items 1-8); b) Pure melt resistivity as a function of temperature for a range of plausible values of explored parameters; c) Bulk resistivity of partially molten rock as a function of melt fraction. The figures are adapted from (Kaufl et al., 2020) and (Comeau et al., 2018).

APPENDIX E:

MT MODELS AND CORRESPONDING INFORMATION MONGOLIAN MT PAPERS

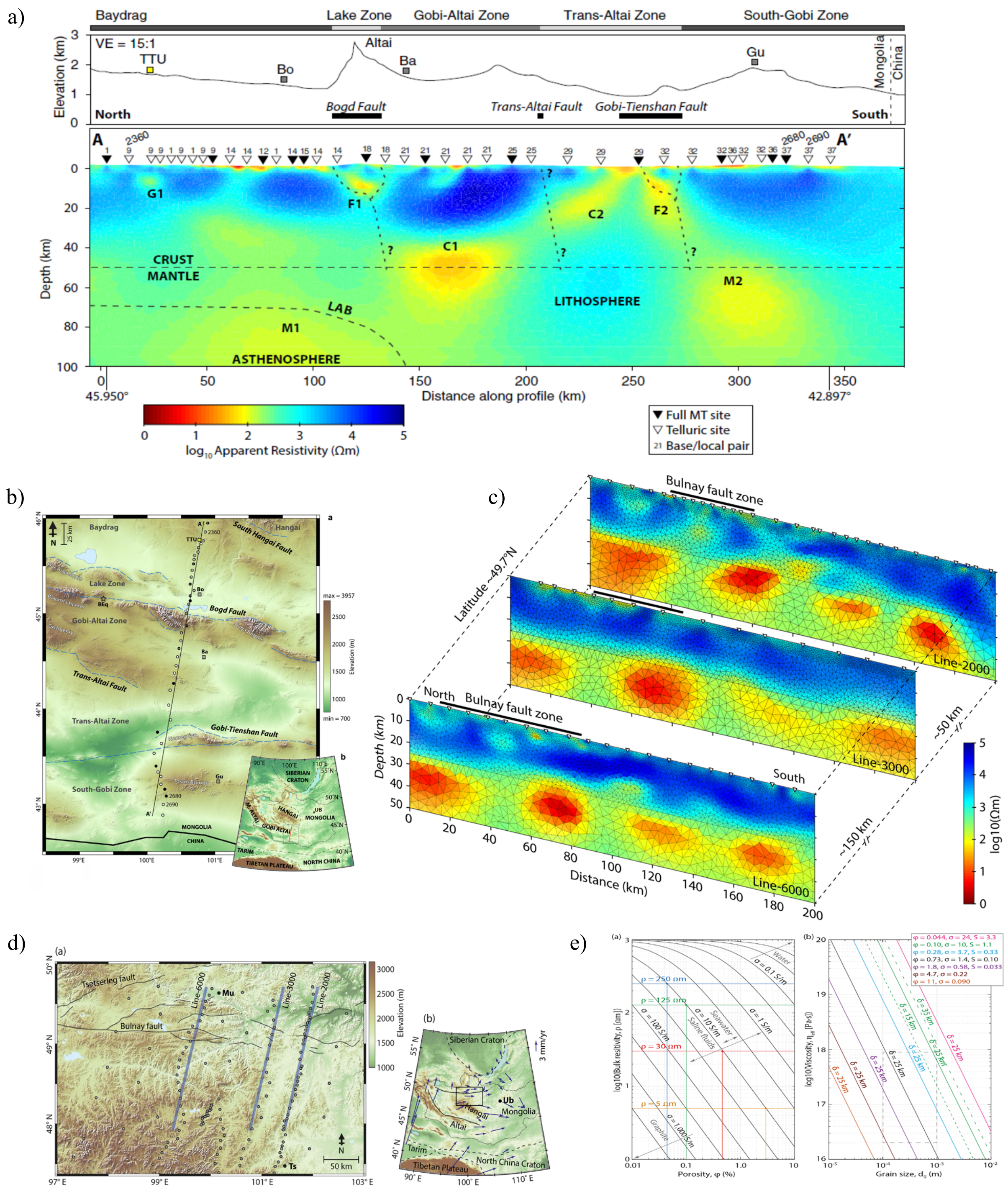

Fig. E2. a) The 2-D electrical resistivity model of southern Mongolia, which crosses several fault zones/terrane boundaries shown in panel b); here, F1-F2 are the fault-related conductors, C1-C2 are the crustal conductors, M1-M2 the upper mantle conductors, LAB is Lithosphere Asthenosphere Boundary and G1 is the conductor observed beneath gold deposits; c) Electrical resistivity models obtained from MT data collected along the lines shown in panel d); e) Mechanical characteristics of the recovered models. The figures are adapted from (Comeau et al., 2020a) and (Comeau et al., 2020b).

APPENDIX E:

MT MODELS AND CORRESPONDING INFORMATION MONGOLIAN MT PAPERS

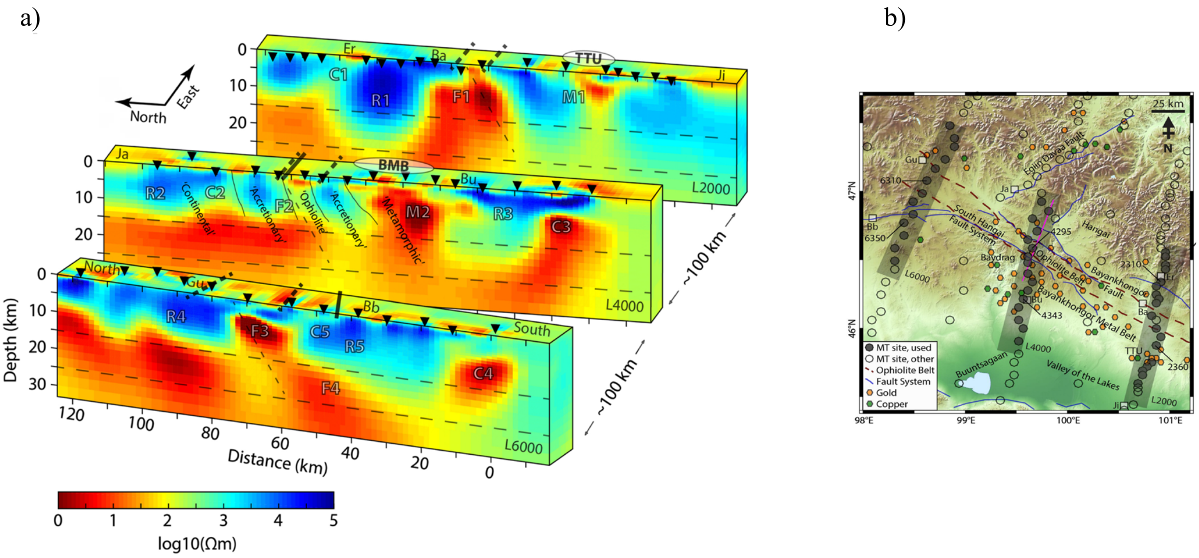

Fig. E3. a) The 3-D electrical resistivity models, which cover shaded rectangles in panel b), where M1-M2 conductors are coincident with the Bayankhongor metallic belt. The figures are adapted from (Comeau et al., 2021a).

APPENDIX E:

MT MODELS AND CORRESPONDING INFORMATION MONGOLIAN MT PAPERS

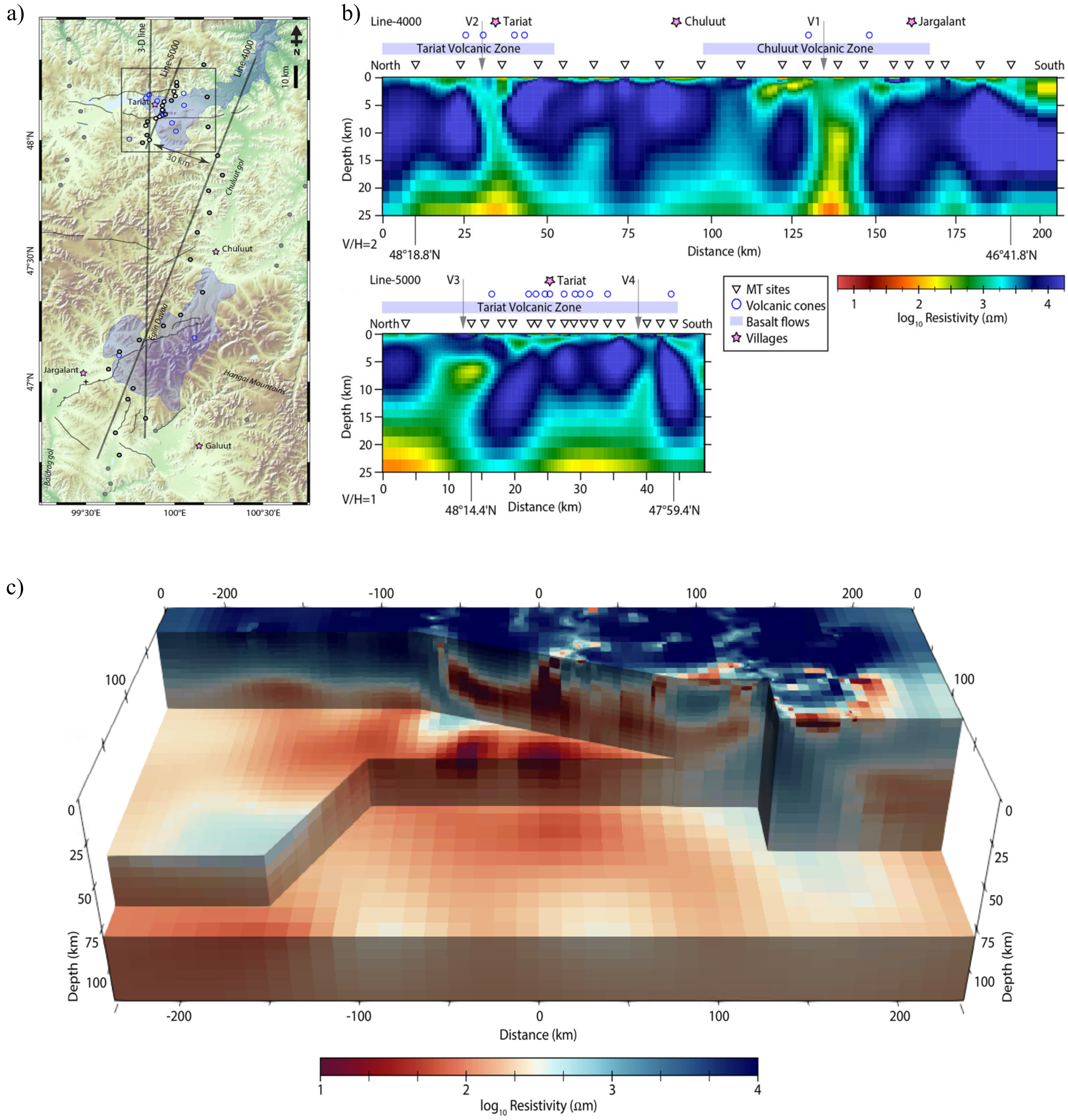

Fig. E4. a) and b) The survey area and electrical resistivity model of the volcanic zones in the central Khangai; c) Cutaway of the 3-D resistivity model presumably showing fossil fluid pathways in the Bayankhongor metallic belt. The figures are adapted from (Comeau et al., 2022a) and (Comeau et al., 2022b).

APPENDIX E:

MT MODELS AND CORRESPONDING INFORMATION MONGOLIAN MT PAPERS

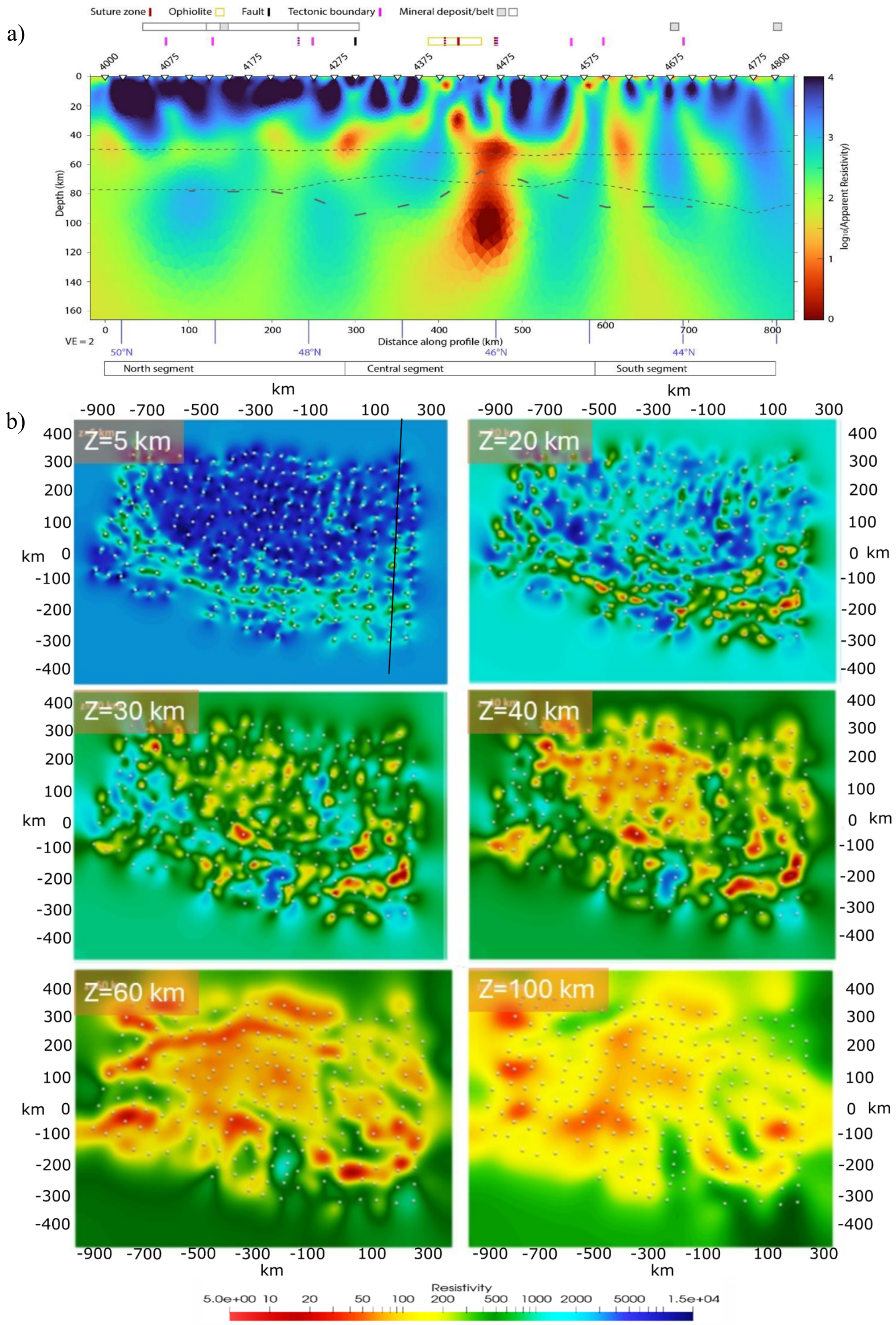

Fig. E5. a) The 2-D resistivity model along the profile shown by the black line at the 5 km depth slice of panel b); b) The horizontal slices (at different depths) of the 3-D electrical resistivity model across Mongolia. The figures are adopted from (Comeau et al., 2024a) and (Rigaurd, 2024)

APPENDIX E:

MT MODELS AND CORRESPONDING INFORMATION MONGOLIAN MT PAPERS

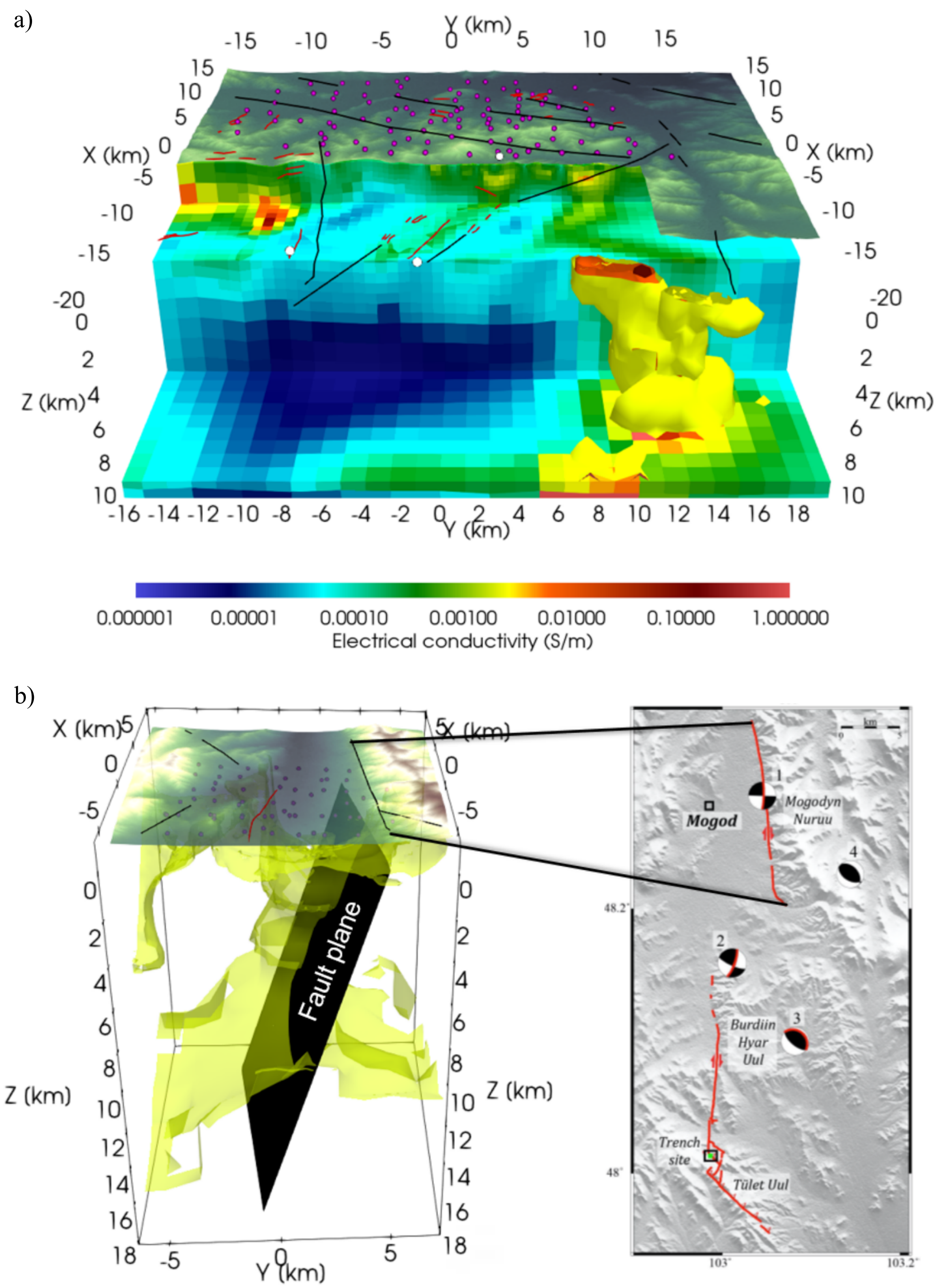

Fig. E6. a) Cutaway of the 3-D conductivity models of the Tsenkher; b) Cutaway of the 3-D conductivity models of the Mogod. The figures are adopted from (Enkhzul et al., 2022)